

A 2-D Numerical Model for Linear Long Wave Propagation in Boundary-fitted Curvilinear Grids

Sevil Deniz Yakan¹, Çiğdem Akan² and Serdar Beji³

SUMMARY

In this paper, vertically integrated linearized long wave equations are numerically solved in a boundary-fitted curvilinear grid. The equations are first expressed in the generalized non-orthogonal curvilinear co-ordinates. The cartesian velocity vectors are also replaced by the contravariant velocity vectors by appropriate combinations of the transformed momentum equations. The governing equations in the transformed space are solved in a rectangular mesh of the computational grid system. The boundary conditions which are taken into consideration are incoming boundary condition, wall condition and outgoing boundary condition. Fischer's numerical scheme based on a staggered grid (Arakawa-C) system is applied to the governing equations in the generalized curvilinear coordinates. For a test case linear wave propagation in a circular shaped channel is carried out.

1. INTRODUCTION

In order to solve the two-dimensional (2D) depth-integrated shallow water equations, finite difference method (FDM) is usually preferred due to its simplicity and effectiveness. Notwithstanding, for shallow water problems, traditional finite difference model has definite shortcomings when applied to complicated regions. Owing to the fact that the stepwise representation of a curved lateral geometry in Cartesian grid is only a crude approximation, the computational results from a uniform Cartesian grid are not much reliable [1]. To prevent this handicap, curvilinear grid methods are used so that boundary conditions on curved boundaries can be satisfied more accurately [5].

In boundary-fitted curvilinear grid models, the physical curved region is transformed onto a simpler rectangular computational domain by transforming governing equations of flow, and then the finite difference method is applied to these governing equations. The complexity of the resulting equations is basically related to the order of derivatives present in the original Cartesian equations. Although non-orthogonal co-ordinate transformation is the most complex transformation, it has the advantage of having least restricted mesh distribution hence the highest flexibility of use [5]. In this approach, the contravariant components of the velocity vector are used as generalized components of velocity in the transformed image domain. Shi et. al. (1997) used the transformed shallow water equations in terms of contravariant velocity components to model storm surge. Later, the Boussinesq equations in generalized coordinates were solved by Shi et. al. (2001).

The coordinate transformations may basically be accomplished in two different ways. In the first method,

primitive variables (u , v , eta) are remained unchanged while only the independent variables are transformed. In this case the transformation may be accomplished easily but the equations and the boundary conditions are more complex. The second method, on the other hand, makes use of the normal components of the velocity vector in curvilinear co-ordinates or the covariant components of the velocity vector in the curvilinear co-ordinate system (Warsi, 1998). The obtained equations and the boundary conditions are much simpler compared with the first method [6].

By using boundary-fitted curvilinear co-ordinate transformation, the applicability of conventional finite difference methods can be extended to complex geometries [8]. Additionally, using structured curvilinear grids with finite difference discretizations allows programming simplicity. Especially for complicated geometries, such as harbours and tidal inlets the curvilinear grids pose a real advantage over rectangular grids which use a steplike representation of the boundaries [6].

Recently, for the simulation of the circulation in marine and estuarine regions, curvilinear co-ordinates are commonly used. ECOM (Estuarine, Coastal and Ocean Model) and POM (Princeton Ocean Model) utilized orthogonal curvilinear grids in the horizontal directions and sigma-stretched grids in the vertical direction. Nevertheless, for most estuarine and coastal applications, due to complex geometries of coastlines, the orthogonal grids can not be generated unless the coastline is approximated with simple curves. Generalized curvilinear grids should necessarily be preferred for a better fit to lateral boundaries and for more accurate simulations [1].

¹ Department of Naval Architecture and Ocean Engineering; Istanbul Technical University; Maslak 34469; Istanbul; Turkey
Phone: +90 212 285 6397 Fax: +90 212 285 6454 e-mail: yakans@itu.edu.tr

² Department of Naval Architecture and Ocean Engineering; Istanbul Technical University; Maslak 34469; Istanbul; Turkey
Phone: +90 212 285 6426 Fax: +90 212 285 6454 e-mail: akanc@itu.edu.tr

³ Department of Naval Architecture and Ocean Engineering; Istanbul Technical University; Maslak 34469; Istanbul; Turkey
Phone: +90 212 285 6442 Fax: +90 212 285 6454 e-mail: sbeji@itu.edu.tr

2. GOVERNING EQUATIONS

In rectangular Cartesian co-ordinates, the linearized continuity equation and x - and y - components of the momentum equation are given as

$$\frac{\partial(hu)}{\partial x} + \frac{\partial(hv)}{\partial y} = -\frac{\partial\zeta}{\partial t} \quad (1)$$

$$\frac{\partial u}{\partial t} + g\frac{\partial\zeta}{\partial x} = 0 \quad (2)$$

$$\frac{\partial v}{\partial t} + g\frac{\partial\zeta}{\partial y} = 0 \quad (3)$$

where ζ is the free surface elevation, u and v are the Cartesian components of the horizontal velocity vector at still water level at $z = 0$, g is the gravitational acceleration.

Due to the complex shapes of computational fields, it can be necessary to express governing equations in a special co-ordinate system. Boundary-fitted grids are mostly used to calculate flow in such complex geometries. Being adoptable to any geometry is the main advantage of such grids. Since the grid lines follow the boundaries, the boundary conditions are easily implemented.

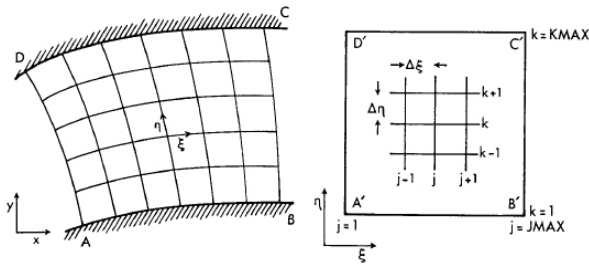


Figure 1. Physical and computational domain.

Co-ordinate transformations from a two-dimensional Cartesian system (x,y,t) to a two-dimensional curvilinear system (ζ,η,τ) are given as

$$\frac{\partial}{\partial x} = \xi_x \frac{\partial}{\partial \xi} + \eta_x \frac{\partial}{\partial \eta}$$

$$\frac{\partial}{\partial y} = \xi_y \frac{\partial}{\partial \xi} + \eta_y \frac{\partial}{\partial \eta} \quad (4)$$

$$\frac{\partial}{\partial t} = \frac{\partial}{\partial \tau}$$

where the metrics of the transformation are defined as

$$\xi_x = Jy_\eta, \quad \xi_y = -Jx_\eta,$$

$$\eta_x = -Jy_\xi, \quad \eta_y = Jx_\xi \quad (5)$$

and the Jacobian of the transformation is

$$J = \frac{1}{(x_\xi y_\eta - x_\eta y_\xi)} \quad (6)$$

Denoting the contravariant velocity components in the ξ - and η -directions by U and V gives

$$u_x + u_y = J(U_\xi^* + V_\eta^*) \quad (7)$$

where U^* and V^* are defined as $U^* = U/J$, $V^* = V/J$. The wave model in curvilinear co-ordinates in terms of contravariant velocity components becomes

$$\frac{1}{J} \frac{\partial}{\partial \tau} (U^*) + g \frac{1}{J^2} (\xi_x^2 + \xi_y^2) \frac{\partial \zeta}{\partial \xi}$$

$$+ g \frac{1}{J^2} (\xi_x \eta_x + \xi_y \eta_y) \frac{\partial \zeta}{\partial \eta} = 0 \quad (8)$$

$$\frac{1}{J} \frac{\partial}{\partial \tau} (V^*) + g \frac{1}{J^2} (\xi_x \eta_x + \xi_y \eta_y) \frac{\partial \zeta}{\partial \xi}$$

$$+ g \frac{1}{J^2} (\eta_x^2 + \eta_y^2) \frac{\partial \zeta}{\partial \eta} = 0 \quad (9)$$

$$\zeta_\tau + J \left[hU^* \right]_\xi + J \left[hV^* \right]_\eta = 0 \quad (10)$$

3. BOUNDARY CONDITIONS

Boundary conditions used to visualize this model are incoming boundary condition, wall condition, and outgoing boundary condition.

The incoming boundary is taken along the η -axis at $\xi = 0$. Because the grids always fit the physical boundary, the boundary condition can be accurately described. Thus, the method can improve the accuracy of simulation and make the numerical scheme convenient [1].

Due to the wall condition, the contravariant velocity components normal to the wall boundaries becomes zero:

$$U^* = 0 \quad \text{and} \quad V^* = 0 \quad (11)$$

Radiation condition ensures the propagation of waves without any reflection at the outgoing boundary. Sommerfeld's radiation condition is given as

$$u_t \pm Cu_x = 0 \quad (12)$$

4. NUMERICAL PROCEDURE

4.1. GRID ORIENTATION

In the numerical application, staggered Arakawa C-grid is used and the grid orientations for the variables of transformed equations are shown separately in Figures 2, 3 and 4, and together in Figure 5.

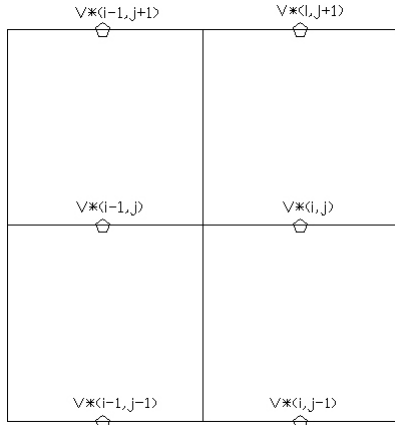


Figure 2. Grid orientation for variable V^*

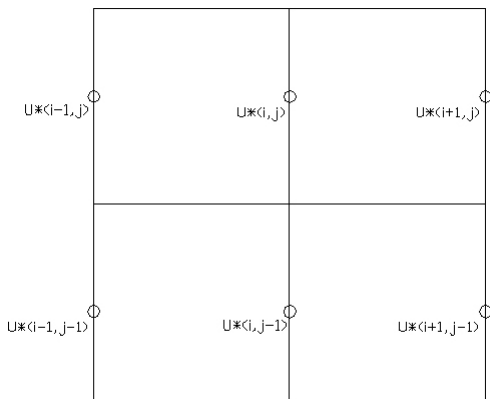


Figure 3. Grid orientation for variable U^*

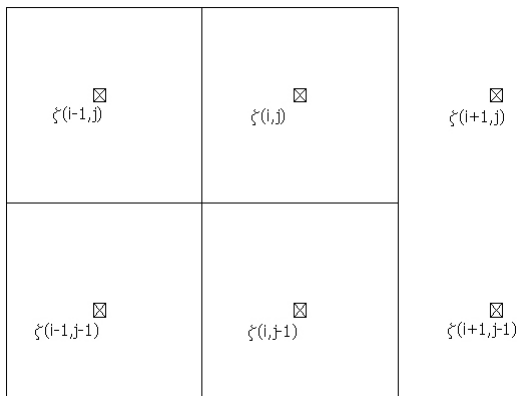


Figure 4. Grid orientation for variable ζ

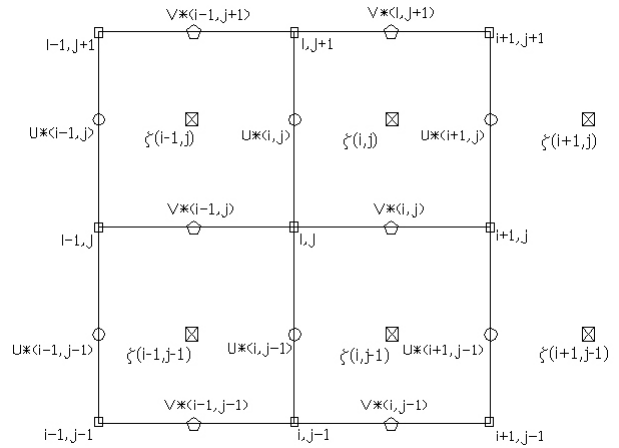


Figure 5. Grid orientation for all variables

4.2. DISCRETIZATION OF CONTINUITY EQUATION

Continuity equation in curvilinear coordinates is expressed as with Equation (14), where U^* and V^* are components of the horizontal velocity component at the still water at $z = 0$ along the ζ - and η - directions respectively.

After imposing the Fischer algorithm, continuity equation becomes

$$\frac{\zeta_{i,j}^{k+2} - \zeta_{i,j}^k}{2\Delta t} = -J \left[\begin{aligned} & \left(\frac{h_{i+1,j} + h_{i+1,j+1}}{2} \right) U_{i+1,j}^{*k+1} \\ & - \left(\frac{h_{i,j} + h_{i,j+1}}{2} \right) U_{i,j}^{*k+1} \\ & - J \left[\begin{aligned} & \left(\frac{h_{i,j+1} + h_{i+1,j+1}}{2} \right) V_{i,j+1}^{*k+1} \\ & - \left(\frac{h_{i,j} + h_{i+1,j}}{2} \right) V_{i,j}^{*k+1} \end{aligned} \right] \end{aligned} \right] \quad (13)$$

where i and j indices are abscises and ordinates according to ζ and η -axes, k is the number of time step, Δt is the time step, $\Delta \zeta$ shows the step along the ζ -axis and $\Delta \eta$ is the step along the η -axis. In addition, for the ease of the calculation, $\Delta \zeta = \Delta \eta = 1$ is taken.

4.3. DISCRETIZATION OF MOMENTUM EQUATIONS

Discretization of ζ component of the momentum equation gives the U^* values at the new time step and discretization of η component of the momentum equation gives the V^* values at the new time step as shown below

$$\begin{aligned} \frac{U_{i,j}^{*k+2} - U_{i,j}^{*k}}{2\Delta t} = & -g \frac{1}{J} \left(\xi_x^2 + \xi_y^2 \right) \left(\zeta_{i,j}^{k+1} - \zeta_{i-1,j}^{k+1} \right) \\ & -g \frac{1}{J} \left(\xi_x \eta_x + \xi_y \eta_y \right) \\ & \left(\zeta_{i,j+1}^{k+1} - \zeta_{i,j-1}^{k+1} + \zeta_{i-1,j+1}^{k+1} \right. \\ & \left. - \zeta_{i-1,j-1}^{k+1} \right) \end{aligned} \quad (14)$$

$$\begin{aligned} \frac{V_{i,j}^{*k+2} - V_{i,j}^{*k}}{2\Delta t} = & -g \frac{1}{J} \left(\eta_x^2 + \eta_y^2 \right) \left(\zeta_{i,j}^{k+1} - \zeta_{i,j-1}^{k+1} \right) \\ & -g \frac{1}{J} \left(\xi_x \eta_x + \xi_y \eta_y \right) \\ & \left(\zeta_{i+1,j}^{k+1} - \zeta_{i-1,j}^{k+1} + \zeta_{i+1,j-1}^{k+1} \right. \\ & \left. - \zeta_{i-1,j-1}^{k+1} \right) \end{aligned} \quad (15)$$

where

$$\begin{aligned} \eta_x = -J \frac{y_{i+1,j} - y_{i-1,j}}{2\Delta\eta}, \quad \eta_y = J \frac{x_{i+1,j} - x_{i-1,j}}{2\Delta\eta}, \\ \xi_x = J \frac{y_{i,j+1} - y_{i,j-1}}{2\Delta\xi}, \quad \xi_y = -J \frac{x_{i,j+1} - x_{i,j-1}}{2\Delta\xi} \end{aligned} \quad (16)$$

where ξ_x, η_x are the derivatives of ξ and η with respect to x , and ξ_y, η_y are the derivatives of ξ and η with respect to y , and J is the Jacobian given in equation (9).

5. LINEAR LONG WAVE SIMULATION

The transformed continuity and momentum equations in curvilinear co-ordinates are used for the simulation of linear long waves in a circular channel. The circular channel considered is a half circle covering an arc of 180°; the outer and the inner radii of the circular channel are taken as 100 and 60m, respectively. Since the choice of water depth is $h=0.5$ m and the incident wave period $T=7$ s, the wavelength and the wave number parameters are 21m and 0.3 rad/m, respectively. The time resolution is taken as $\Delta t = T / 50$, so that the numerical stability and long wave conditions are satisfied. For numerical stability the Courant number must be less $1/2\sqrt{2}$, and long wave condition requires that the ratio between the water depth and the wavelength be less than $1/20$, which is calculated as 0.032 for the computations performed.

At the entrance of the circular channel, a sinusoidal wave with uniform amplitude is used, and at the end of the

circular channel, Sommerfeld's equation is used as the radiation condition.

Below, the perspective views of the linear long wave propagations are seen for $t=5T$ and $t=10T$, respectively. The reflection and diffraction features of the wave propagation between the inner and outer walls of the circular channel result in complicated propagation paths as seen from the perspective views. Also, the contours of the numerical solution are given from the x-y view.

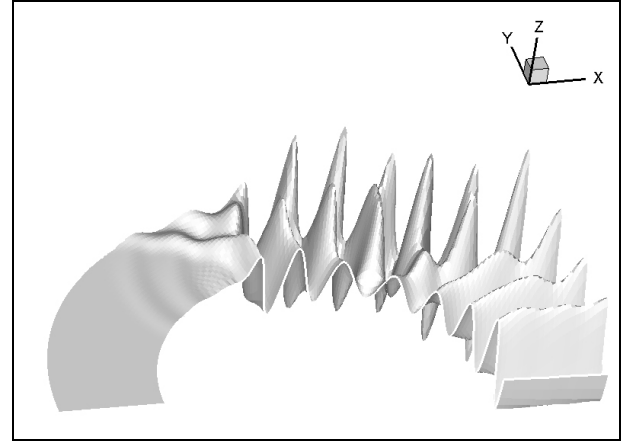


Figure 6. Perspective view for $t = 5T$

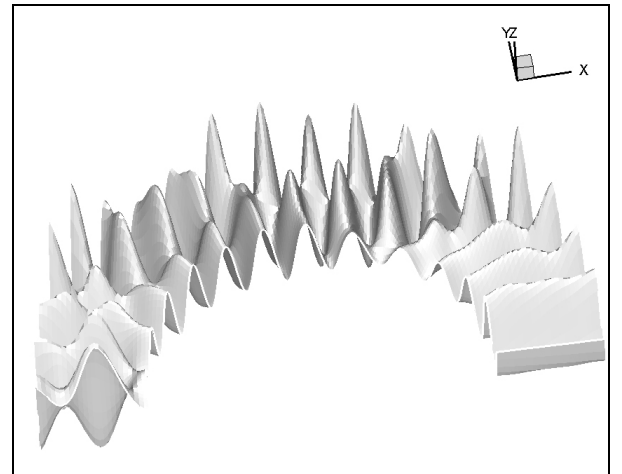


Figure 7. Perspective view for $t = 10T$

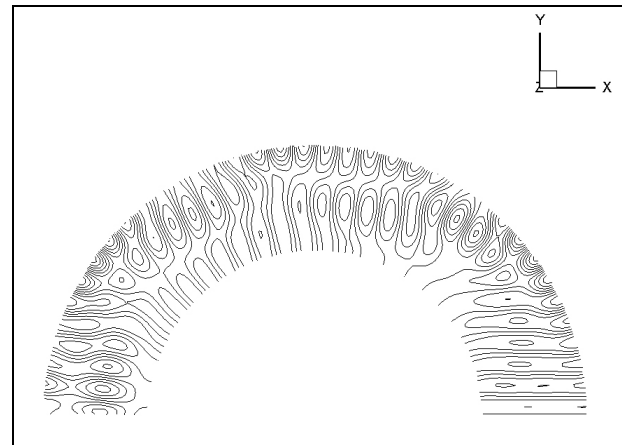


Figure 8. Contours of the numerical solution at $t = 10T$

6. CONCLUSION

In this study, shallow water equations are expressed in generalized curvilinear co-ordinate system in terms of contravariant velocity components. Numerical solution is performed using contravariant velocities and as a result, boundary conditions are expressed in the simplest form. Thus, linear shallow water waves propagating in complex geometries such as marinas, channels, lakes etc., can be simulated more accurately.

REFERENCES

1. BAO, X.W., YAN, J., and SUN, W.X., 'A Three-dimensional Tidal Model in Boundary-fitted Curvilinear Grids', *Estuarine, Coastal and Shelf Science*, 2000.
2. BEJÍ, S., and BARLAS, B., 'Boundary-fitted Non-linear Dispersive Wave Model for Regions of Arbitrary Geometry', *International Journal for Numerical Methods in Fluids*, 2004.
3. FLETCHER, C.A.J., 'Computational Techniques for Fluid Dynamics 2', Springer-Verlag Berlin Heidelberg, 1988.
4. HOFFMAN, K.A., and CHIANG S.T., 'Computational Fluid Dynamics for Engineers, Volume 2', Engineering Education System: Wichita, Kansas, 1995.
5. LIN, B., and CHANDLER-WILDE, S.N., 'A Depth-integrated 2D Coastal and Estuarine Model with Conformal Boundary-fitted Mesh Generation', *International Journal for Numerical Methods in Fluids*, 1996.
6. SHI, F., DALRYMPLE, R.A., KIRBY, J., CHEN, Q. And KENNEDY, A., 'A Fully Nonlinear Boussinesq Model in Generalized Curvilinear Coordinates', *Coastal Engineering*, 2001.
7. SHI, F., SUN, W., and WEI, G., 'A WDM Method on a Generalized Curvilinear Grid for Calculation of Storm Surge Flooding', *Applied Ocean Research*, 1997.
8. YE, J., McCORQUODALE, and PENG, J., 'A Fractional Two-step Implicit Algorithm Using Curvilinear Collected Grids', *International Journal for Numerical Methods in Fluids*, 2006.

